

Observation of Dirac cones and room temperature polariton lasing in an organic honeycomb lattice

Simon Betzold, Johannes Düreth, Marco Dusel, Monika Emmerling, Antonina Bieganowska, Jürgen Ohmer, Utz Fischer, Sven Höfling, and Sebastian Klemmt**

S. Betzold, J. Düreth, M. Dusel, M. Emmerling, S. Höfling, S. Klemmt

Julius-Maximilians-Universität Würzburg, Physikalisches Institut and Würzburg-Dresden Cluster of Excellence ct.qmat, Lehrstuhl für Technische Physik, Am Hubland, 97074 Würzburg, Germany

A. Bieganowska

Wroclaw University of Science and Technology, Faculty of Fundamental Problems of Technology, Department of Experimental Physics, Wyb. Wyspiańskiego 27, 50-370 Wroclaw, Poland

J. Ohmer, U. Fischer

Julius-Maximilians-Universität Würzburg, Department of Biochemistry, Am Hubland, 97074 Würzburg, Germany

*E-mail: simon.betzold@uni-wuerzburg.de, sebastian.klemmt@uni-wuerzburg.de

Keywords: Microcavities; Polariton laser; Optical lattices; Organic Semiconductors; Quantum Simulation;

Artificial one- and two-dimensional lattices have emerged as a powerful platform for the emulation of lattice Hamiltonians, the fundamental study of collective many-body effects as well as phenomena arising from non-trivial topology. Exciton-polaritons, bosonic part-light and part-matter quasiparticles, combine pronounced nonlinearities with the possibility of on-chip implementation. In this context, organic semiconductors, hosting ultra-stable Frenkel excitons, embedded in a microcavity have proven to be versatile contenders for the study of nonlinear many-body physics and bosonic condensation, which also enable deployment at ambient conditions. Here, we implement a well-controlled, high-quality optical lattice, hosting light-matter quasi-particles. The realized polariton graphene presents with excellent cavity quality factors, showing distinct

signatures of Dirac cone and flatband dispersions as well as polariton lasing at room temperature. This is realized by filling coupled dielectric microcavities with the fluorescent protein mCherry. We demonstrate the emergence of a coherent polariton condensate at ambient conditions, profiting from coupling conditions as precise and controllable as in state-of-the-art inorganic semiconductor-based systems, without limitations due to e.g. lattice matching in epitaxial growth. This progress allows straightforward extension to more complex systems, such as the study of topological phenomena in two-dimensional lattices including topological lasers and non-Hermitian optics.

1. Introduction

Increasing technological control over the past decade has allowed for ever more sophisticated implementations of artificial lattice systems for the investigation and exploration of novel and exciting states of matter^[1,2] as well as the experimental emulation of complex lattice Hamiltonians.^[3] Drawing inspiration from exciting results in the field of ultracold atoms^[4,5] and ion traps,^[6] coupled optical lattices have emerged as a comparatively simple, on-chip platform for lattice emulation^[7-9]. In this context, coupled high-quality vertical resonator microcavities are widely utilized as a precise and well controlled optical platform for lattice emulation and the realization of complex lattice Hamiltonians.^[10-12] Placing a suitable emitter material between two highly reflective mirrors, the emission and reabsorption of light can become dominant, resulting in a strong coupling of light and matter. Because of this, new eigenstates, called exciton-polaritons (polaritons) emerge.^[13,14] Interestingly, they inherit large optical nonlinearities from their matter part, while maintaining a low effective mass and great experimental access from their light part. Landmark results in this system include Bose-Einstein condensation,^[15,16] superfluidity^[17] or electrically pumped polariton laser devices.^[18] Placing such *quantum fluids of light*^[19] in an optical lattice potential landscape using a variety of techniques^[11] has led to the realization of lasing from a topological defect,^[20,21] the implementation of a spin *XY*-Hamiltonian,^[12] as well as the fabrication of polariton graphene^[22-25] including the realization of a polariton topological Chern insulator.^[26] The main material platform traditionally has been high-quality GaAs-based crystalline semiconductor microcavities, benefitting from a very mature epitaxial growth and nanofabrication.^[11] While the platform allows even for electrical operation of polariton devices,^[18,25,27,28] the fabrication required state-of-the-art clean room facilitates and operation is typically limited to cryogenic temperatures.

Novel emitter materials such as organic emitters,^[29-32] transition metal dichalcogenides^[33-36] and perovskites^[37-40] have been successfully introduced into optical (dielectric) microcavities, adding a comparatively simple fabrication process as well as room temperature stable excitons to the equation. While respectable attempt towards the realization of two-dimensional polariton lattices hosting room temperature emitter materials have been made^[41-43], the combination of a versatile platform with high quality factor (narrow linewidth), low disorder and tunable and controllable inter-site couplings remains challenging.

In this work, we present a high-quality two-dimensional polariton lattice hosting an organic emitter material with excitons stable at room temperature. A graphene-like honeycomb lattice is realized by nanofabricating dimples into a borosilicate substrate by focused ion beam milling. The dimple lattice is subsequently oversputtered with layer pairs of SiO₂ and TiO₂ forming a dielectric, highly reflective distributed Bragg reflector (DBR). Lastly, the fluorescent protein mCherry, closely related to the famous green fluorescent protein,^[44] is drop cast onto a planar mirror and sandwiched with the patterned honeycomb mirror. The resulting structure is a high-quality microcavity lattice, confining light between the two mirrors (z-direction). In addition, light is confined in-plane (x,y-direction) by the hemispheric dimple cavities.^[45] Distance and curvature of the dimples are designed in such a way that the inter-site coupling is sizable and the lattice dominated by nearest neighbor coupling. We observe room temperature exciton polaritons in a very well-defined graphene-like band structure displaying Dirac cone dispersions and flatbands, as well as unequivocal observation of polariton lasing.

2. Results

A detailed schematic representation of the fabricated device is shown in **Figure 1a**. It consists of two DBRs, each sputtered on borosilicate glass substrates with a roughness of less than 1 nm RMS, between which a thin film of the fluorescent protein mCherry is sandwiched. Prior to coating the upper substrate with the mirror pairs, focused ion beam milling (FEI Helios NanoLab DualBeam) was used to introduce arrays of hemispheric dimples, arranged in the distinct geometry of a honeycomb lattice. The individual dimples have, depending on the array, diameters between 3 μ m and 5 μ m and depths between 100nm and 300nm. These hemispheres ensure that the light field of the fundamental mode is confined spatially with an effective radius of about \sim 1.0-1.5 μ m. Subsequently, 9 mirror pairs of SiO₂/TiO₂ were applied to the substrate by ion beam sputter deposition (Nordiko 3000). The individual layer thicknesses were chosen so that the stopband center is at a wavelength of $\lambda_C \approx$ 630nm and the first, high-energetic Bragg minimum at 532nm, allowing for efficient laser excitation. A highly concentrated solution

(175 g/l) of mCherry was coated onto the patterned DBR. An identical DBR was deposited on the planar borosilicate glass substrate, which was then flipped onto the mCherry. Finally, the device is dried for 48 hours under a constant pressure of $\sim 0.25 \text{ N/cm}^2$. The structure yields an experimental microcavity Q-factor of 4720 and a Rabi splitting of 198 meV.^[46] To ensure the approximate length of the cavity as well as the two mirrors being parallel, we utilize in-build spacers. The real-space and k-space geometric properties of the honeycomb lattice are shown in **Figure 1b** and **1c**, respectively. The K- and K'-points are prominently connected to the appearance of Dirac cone dispersions in this lattice.^[47] This distinct dispersion is visible in the angle-resolved photoluminescence (PL) measurement displayed in **Figure 1d**. For the measurement we used a 532-nm continuous-wave diode laser which was focused to a Gaussian spot with a size of about $20\mu\text{m}$ in the center of the lattice. In the lowest S-band at approximately $\pm 1.0 \mu\text{m}^{-1}$, the dispersion is well described by a linear crossing of the modes. Above the S-band ranging from $\sim 1.81\text{-}1.83 \text{ eV}$, the P-band and higher order bands are visible. Even small details of the band structure can be well resolved owing to the excellent combination of quality factor and coupling of the lattice.^[23, Fig. 1d]

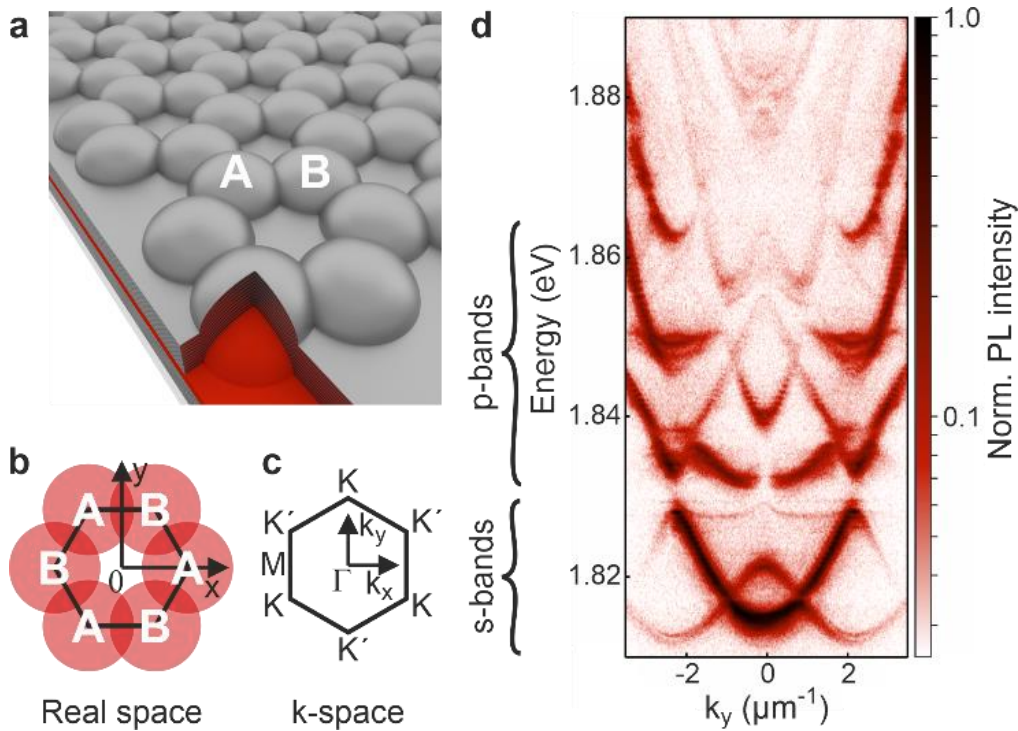


Figure 1. a) Schematic representation of the room-temperature polariton graphene, consisting of the fluorescent protein mCherry sandwiched between a planar and a structured DBR mirror. A and B denote the two-site unit cell of the lattice. b) Schematic representation of the real space lattice as well as c) the geometry in k-space, revealing the K- and K'-points of the lattice. d) Photoluminescence dispersion measurement in K-K' direction.

In order to study the organic room-temperature polariton graphene in more detail, we use a photoluminescence tomographic technique to access the full band structure in the in-plane momentum $k_{x,y}$ and in energy (PL emission wavelength). **Figure 2a-d** show PL dispersion measurements in various high-symmetry directions, referenced in Figure 1c. While in Figure 2a the measurement at $k_x=0 \mu\text{m}^{-1}$ along K- Γ -K' does not present the anti-binding S-band due to destructive interference in the far field, it is well visible in the second Brillouin zone shown in Figure 2b.^[23] Figure 2c displays the dispersion along K-K direction, highlighting the iconic Dirac cone, while the latter is expectedly absent in Figure 2d when measuring along M- Γ -M direction. Due to the fully available k-space dispersion information (within the light cone) we can reconstruct and plot a reduced Brillouin zone in **Figure 2e**. We show the mode energies along the high symmetry points Γ , K/K' and M. The Dirac cone at K and the open bands at M are clearly visible and well described by a tight-binding model considering nearest and next-nearest neighbor coupling (red line). In addition, above the S-band the flatband of the P-mode is visible. It forms due to destructive interference of the overlapping local modes in real space and displays with a vanishing band curvature. **Figure 2f** displays the Dirac cones at the K/K' - points at the intersection energy, similarly to well-known angle-resolved photoemission spectroscopy measurements of graphene^[48] (with μm^{-1} instead of \AA^{-1}) while **Figure 2g** shows the Γ -points of the 2nd Brillouin zones. Similarly to the k-space tomographies, we map the real-space potential landscape by incrementally shifting the image with respect to the entrance slit of our spectrometer, accessing the PL emission energy as a function of (x,y). To make a qualified statement about the homogeneity of the potential landscape, we plot the energy of the anti-binding S-band S_{AB} in **Figure 2h**. As expected for the anti-binding mode the luminescence is located on the individual sites, highlighting the honeycomb pattern. The intensity is homogenous overall, following the Gaussian laser spot excitation with a diameter of approximately $20\mu\text{m}$. Opposed to that the P-flatband mode P_{flat} is located at the contact points of the lattice (as seen in **Figure 2i**) due to the dumbbell shape of the P-mode and the hybridization in the flatband.^[23,49-51] Apart from the emission wavelength of around 685nm, the presenting dispersions compare extremely well with the results achieved at cryogenic temperatures of typically $T=4\text{K}$ in single crystalline III/V-semiconductor based structures.^[23] However, while in coupled micro-resonator pillars the physical overlap of the sites create the coupling, in our lattice the in-plane confinement is caused by the overlapping hemispheres in the top mirror. Taking a closer look at the results in Figure 2, one observes that firstly, the S-band is asymmetric in energy around the Dirac energy of approximately $E_D \sim 1.817 \text{ eV}$, extending more to higher energies than to lower one (cf. Figure 2a-c).

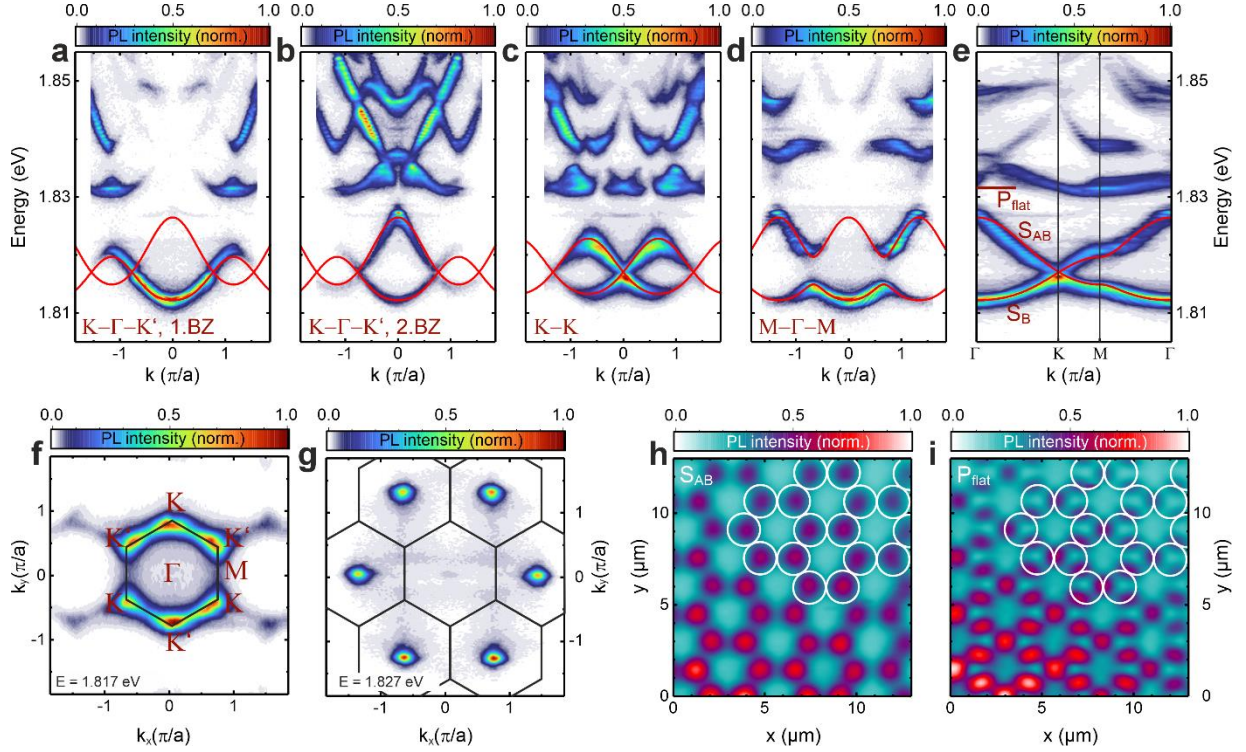


Figure 2. a-d) Polariton dispersions along the K- Γ -K' (first and second Brillouin zone), K-K and M- Γ -M directions of the Brillouin zone. e) Representation of the reduced zone scheme calculated by averaging the first as well as an adjacent second Brillouin zone. f-g) Iso-energy cuts of the Fourier space at the energy of the Dirac cones at 1.817 eV (f) and at the energy of the top of the π^* -Band at 1.827 eV (g), which shows the occupation of the Γ -points in the second Brillouin zone. h-i) Real space images of the anti-bonding S sub-band (h) and of the lowest P sub-band (i).

Secondly, some modulation of the flatband in Figure 2e can be observed. Both signatures arise from next nearest neighbor coupling, common to proximity coupled systems. The energy of a tight-binding model of a Honeycomb lattice is given by

$$E(k) = \pm t_1 \cdot \sqrt{r + f(k)} - t_2 \cdot f(k) \quad (1)$$

where k is the in-plane wave vector and $f(k)$ the geometric function

$$f(k) = 2 \cdot \cos(\sqrt{3}k_y a) + 4 \cos\left(\frac{\sqrt{3}}{2}k_y a\right) \cos\left(\frac{3}{2}k_x a\right). \quad (2)$$

The coefficients t_1 and t_2 are associated with the relative strength of the nearest neighbor coupling t_1 to the next nearest neighbor coupling t_2 . Fitting the dispersions, we end up with $t_2/t_1=0.25\text{meV}/2.38\text{meV}=11\%$. It is now worthwhile to compare this result to existing ones in more conventional inorganic semiconductor based polariton lattices. **Table 1** displays the tight-binding coupling data for several polariton lattices where all compared works have honeycomb geometries. It turns out that, although the resonator designs and the absolute coupling strengths differ, the ratio between next-nearest neighbor coupling t_2 and nearest neighbor coupling t_1 is very comparable in all configurations and material systems. This shows that our hemispherical microcavities are also competitive to established III-V based microcavities in this respect.

Table 1. Comparison of the tight binding coupling parameters of the present work with those existing in conventional inorganic semiconductor cavities.

	t_1 (meV)	t_2 (meV)	t_2/t_1	Confinement technique
This work	2.38	0.25	0.11	Hemispheric top mirror
PhD Thesis Tristan H. Harder ^{a)}	0.356	0.044	0.12	Etch-and-overgrowth technique
Jacqmin et al. ^[23]	0.25	0.02	0.08	Conventional pillar etching
Real et al. ^[52]	0.18	0.014	0.08	Conventional pillar etching
Whittaker et al. ^[24]	0.12	0.008	0.07	Conventional pillar etching

^{a)}publication in preparation, see [53] for the PhD thesis.

This characteristic and the remarkable stability exhibited by Frenkel excitons in fluorescent proteins sets the stage for exploring the nonlinear regime of polariton lasing in 2D lattices at room temperature, as demonstrated in our subsequent experiment. For this we excite the Honeycomb lattice again using a Gaussian spot with a diameter of approximately 20 μm . However, a wavelength-tunable optical parametric oscillator system, utilizing nanosecond pulses, is now employed. This system is specifically tuned to 532 nm to be resonant with the first Bragg minimum of the top mirror in our sample. As we systematically increase the pump power from $P = 0.12\mu\text{J}/\text{pulse}$ (**Figure 3a**) to $P = 0.27\mu\text{J}/\text{pulse}$ (**Figure 3b**), and finally to $P = 1.89\mu\text{J}/\text{pulse}$ (**Figure 3c**), a notable qualitative change in the lattice spectrum is observed. First, a substantial nonlinear enhancement in the emission intensity is identified, concentrated within the spectral region of the d-bands in our lattice. A nonlinear increase of the integrated intensity shown in **Figure 3e** (black dots) by three orders of magnitude is observed. Moreover, Figure

3e reveals a significant reduction in the linewidth at the polariton condensation threshold $P_{th} \approx 0.3\mu\text{J}/\text{pulse}$, indicating the build-up of phase coherence. Lastly, **Figure 3d** illustrates a persistent blueshift of the mode above the threshold which results from phase-space filling effects^[54,55] and is attributed to the exciton-polariton nature of the system, resulting in an overall shift of approximately 0.6meV.

To further explore the spatial coherence of this mode, we investigate its correlation function $g^{(1)}$. Using a Michelson interferometer in a mirror-retroreflector configuration, we overlap the real-space luminescence from the device with its mirror image on a beam splitter, combining them on a high-resolution CCD camera. This measurement is conducted well above threshold with an excitation power of about $P \approx 7P_{th}$. **Figure 3f** shows the resulting interference image where a distinct interference pattern can be observed exhibiting significant spatially extended fringes, characteristic of an extended coherent mode. The spatially resolved magnitude of the coherence measurement shown in **Figure 3g** confirms that the coherent part extends over several unit cells, exceeding more than $10\mu\text{m}$. These results not only demonstrate the potential of polariton lasing in our system, but also underscore the spatially extensive coherence of the emergent coherent mode. The observed effects, including nonlinear enhancement, linewidth reduction, and persistent blueshift, contribute to a comprehensive understanding of the intricate exciton-polariton dynamics in our lattice. This level of control and coherence in a room temperature environment opens new avenues for practical applications and further advances in the study of nonlinear phenomena in condensed matter physics.

3. Conclusion

In this paper, we have successfully demonstrated a versatile platform to bring the physics of photonic lattices in general and polaritonic lattices specifically to the realm of room temperature. We use an organic emitter material that hosts room temperature stable excitons to demonstrate polariton lasing in a complex potential landscape. The geometry of choice is the honeycomb lattice because it draws exciting connections to the emulation of graphene physics, topological insulators and lasers, flatband physics and many more. The use of dielectric mirrors makes this approach fully independent from material restrictions as long as the emission wavelength and the mirror stopband match. While our experiments have been successfully performed on cavities where the emitter is sandwiched between the mirrors, this platform can readily be expanded to open cavity approaches^[56,57], enabling unprecedented freedom in the tuning and deterministic manipulation of research platforms and novel optoelectronic devices.

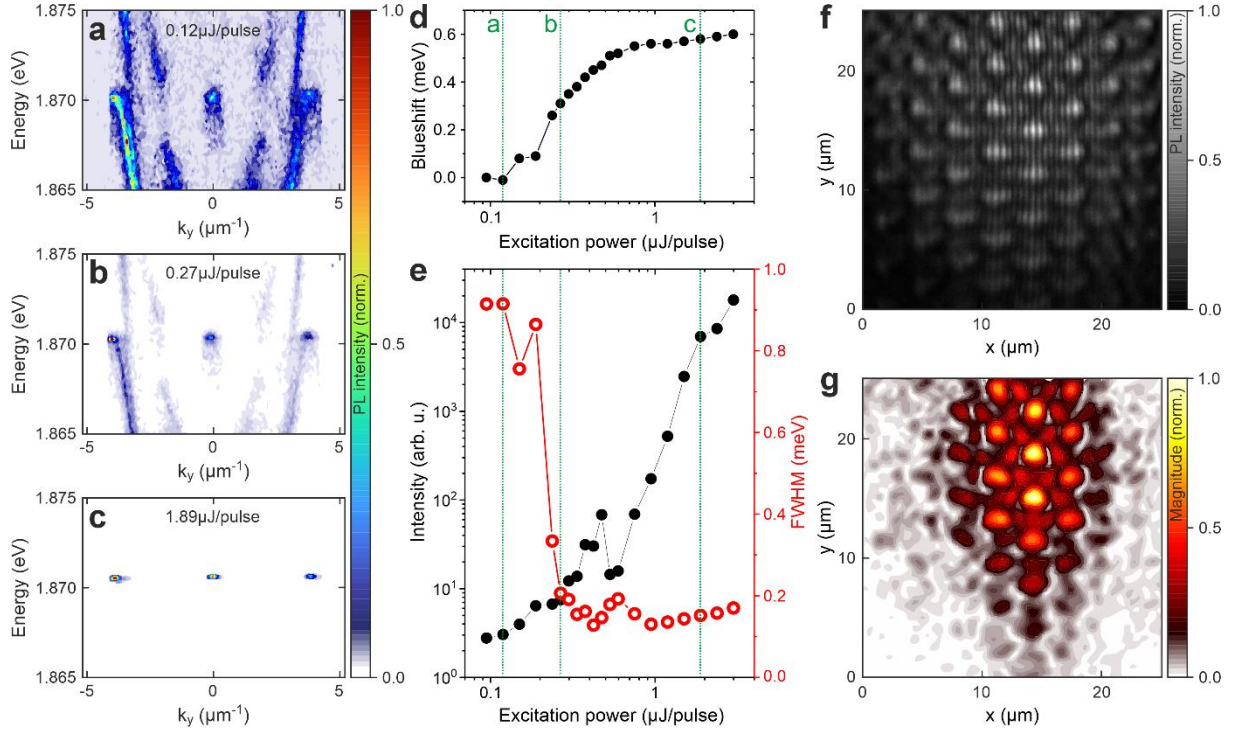


Figure 3. Polariton dispersions of the D-bands along the K-M-K' direction below the condensation threshold (a), at the threshold (b) and well above the condensation threshold (c) under pulsed excitation. D) presents the resulting energy shift for different excitation powers, while e) shows the corresponding input-output characteristics (black) and the linewidth (red). F) Michelson interference image of the polariton condensate at an excitation power of $\sim 2\mu\text{J}/\text{pulse}$ as well as the corresponding spatial $g^{(1)}$ -coherence map in (g), showing a spatial coherence well exceeding $10\mu\text{m}$ and therefore several unit cells.

Acknowledgements

S.B., J.D., M.D., M.E, S.H., and S.K. acknowledge financial support by the German Research Foundation (DFG) under Germany's Excellence Strategy–EXC2147 “ct.qmat” (project id 390858490) and HO 5194/12-1.

References

- [1] G. B. Jo, J. Guzman, C. K. Thomas, P. Hosur, A. Vishwanath, and D. M. Stamper-Kurn, Ultracold atoms in a tunable optical kagome lattice, *Phys. Rev. Lett.* **2012**, *108*, 045305.
- [2] L. Tang, D. Song, S. Xia, S. Xia, J. Ma, W. Yan, Y. Hu, J. Xu, D. Leykam, and Z. Chen, Photonic flat-band lattices and unconventional light localization, *Nanophotonics* **2020**, *9*, 1161-1176.
- [3] M. Polini, F. Guinea, M. Lewenstein, H. C. Manoharan, and V. Pellegrini, Artificial honeycomb lattices for electrons, atoms and photons, *Nature nanotechnology* **2013**, *8*, 625-633 (2013).
- [4] I. Bloch, J. Dalibard, and W. Zwerger, Many-body physics with ultracold gases, *Rev. Mod. Phys.* **2008**, *80*, 885.
- [5] F. Schäfer, T. Fukuhara, S. Sugawa, Y. Takasu, and Y. Takahashi, Tools for quantum simulation with ultracold atoms in optical lattices, *Nature Reviews Physics* **2020**, *2*, 411–425.
- [6] R.C. Sterling, H. Rattanasonti, S. Weidt, K. Lake, P. Srinivasan, S.C. Webster, M. Kraft, and W.K. Hensinger, Fabrication and operation of a two-dimensional ion-trap lattice on a high-voltage microchip, *Nat. Commun.* **2014**, *5*, 3637.
- [7] D. N. Neshev, T. J. Alexander, E. A. Ostrovskaya, Y. S. Kivshar, H. Martin, I. Makasyuk, and Z. Chen, Observation of Discrete Vortex Solitons in Optically Induced Photonic Lattices, *Phys. Rev. Lett.* **2004**, *92*, 123903.
- [8] I. L. Garanovich, S. Longhi, A. A. Sukhorukov, and Y. S. Kivshar, Light propagation and localization in modulated photonic lattices and waveguides, *Physics Reports* **2012**, *518*, 1-79.
- [9] L. Tang, D. Song, S. Xia, S. Xia, J. Ma, W. Yan, Y. Hu, J. Xu, D. Leykam and Z. Chen, Photonic flat-band lattices and unconventional light localization, *Nanophotonics* **2020**, *9*, 1161-1176.
- [10] A. Amo and J. Bloch, Exciton-polaritons in lattices: A non-linear photonic simulator, *C. R. Physique* **2016**, *17*, 934.
- [11] C. Schneider, K. Winkler, M. D. Fraser, M. Kamp, Y. Yamamoto, E. A. Ostrovskaya, and S. Höfling, Exciton-Polariton Trapping and Potential Landscape Engineering, *Rep. Prog. Phys.* **2017**, *80*, 016503.
- [12] N. G. Berloff, M. Silva, K. Kalinin, A. Askitopoulos, J. D. Töpfer, P. Cilibrizzi, W. Langbein, and P. G. Lagoudakis, Realizing the classical XY Hamiltonian in polariton simulators, *Nat. Mater.* **2017**, *16*, 1120– 1126.

- [13] C. Weisbuch, M. Nishioka, A. Ishikawa, and Y. Arakawa, Observation of the coupled exciton-photon mode splitting in a semiconductor quantum microcavity. *Phys. Rev. Lett.* **1992**, *69*, 3314.
- [14] H. Deng, H. Haug, and Y. Yamamoto, Exciton-polariton Bose-Einstein condensation, *Rev. Mod. Phys.* **2010**, *82*, 1489.
- [15] J. Kasprzak, M. Richard, S. Kundermann, A. Baas, P. Jeambrun, J. M. J. Keeling, F. M. Marchetti, M. H. Szymańska, R. André, J. L. Staehli, V. Savona, P. B. Littlewood, B. Deveaud, and S. LeDang, Bose-Einstein condensation of exciton polaritons, *Nature* **443**, 409–414 (2006).
- [16] R. Balili, V. Hartwell, D. Snoke, L. Pfeiffer, and K. West, Bose–Einstein Condensation of Microcavity Polaritons in a Trap, *Science* **2007**, *316*, 1007– 1010.
- [17] A. Amo, J. Lefrère, S. Pigeon, C. Adrados, C. Ciuti, I. Carusotto, R. Houdré, E. Giacobino, and A. Bramati, Superfluidity of polaritons in semiconductor microcavities, *Nat. Phys.* **2009**, *5*, 805-810.
- [18] C. Schneider, A. Rahimi-Iman, N. Y. Kim, J. Fischer, I. G. Savenko, M. Amthor, M. Lermer, A. Wolf, L. Worschech, V. D. Kulakovskii, I. A. Shelykh, M. Kamp, S. Reitzenstein, A. Forchel, Y. Yamamoto, and S. Höfling, An electrically pumped polariton laser, *Nature* **2013**, *497*, 348–352.
- [19] I. Carusotto and C. Ciuti, Quantum fluids of light, *Rev. Mod. Phys.* **2013**, *85*, 299.
- [20] P. St-Jean, V. Goblot, E. Galopin, A. Lemaître, T. Ozawa, L. LeGratiet, I. Sagnes, J. Bloch, and A. Amo, Lasing in topological edge states of a one-dimensional lattice, *Nat. Photon.* **2017**, *11*, 651–656.
- [21] T. H. Harder, M. Sun, O. A. Egorov, I. Vakulchyk, J. Beierlein, P. Gagel, M. Emmerling, C. Schneider, U. Peschel, I. G. Savenko, S. Klemmt, and S. Höfling, Coherent Topological Polariton Laser, *ACS Photonics* **2021**, *8*, 1377–1384.
- [22] K. Kusudo, N. Y. Kim, A. Löffler, S. Höfling, A. Forchel, Y. Yamamoto, Stochastic Formation of Polariton Condensates in Two Degenerate Orbital States, *Phys. Rev. B*, **2013**, *87*, 214503.
- [23] T. Jacqmin, I. Carusotto, I. Sagnes, M. Abbarchi, D. Solnyshkov, G. Malpuech, E. Galopin, A. Lemaître, J. Bloch, and A. Amo, Direct observation of Dirac cones and a flatband in a honeycomb lattice for polaritons, *Phys. Rev. Lett.* **2014**, *112*, 11.
- [24] C. E. Whittaker, T. Dowling, A. V. Nalitov, A. V. Yulin, B. Royall, E. Clarke, M. S. Skolnick, I. A. Shelykh, and D. N. Krizhanovskii, Optical analogue of Dresselhaus spin–orbit interaction in photonic graphene, *Nat. Phys.* **2021**, *15*, 193-196.

- [25] H. Suchomel, S. Klemmt, T. H. Harder, M. Klaas, O. A. Egorov, K. Winkler, M. Emmerling, R. Thomale, S. Höfling, and C. Schneider, Platform for Electrically Pumped Polariton Simulators and Topological Lasers, *Phys. Rev. Lett.* **2018**, *121*, 257402.
- [26] S. Klemmt, T.H. Harder, O. A. Egorov, K. Winkler, R. Ge, M. A. Bandres, M. Emmerling, L. Worschech, T. C. H. Liew, M. Segev, C. Schneider, and S. Höfling, Exciton-polariton topological insulator, *Nature* **2018**, *562*, 552–556.
- [27] S. I. Tsintzos, N. T. Pelekanos, G. Konstantinidis, Z. Hatzopoulos, and P. G. Savvidis, A GaAs polariton light-emitting diode operating near room temperature, *Nature* **2008**, *453*, 372-375.
- [28] P. Gagel, T. H. Harder, S. Betzold, O. A. Egorov, J. Beierlein, H. Suchomel, M. Emmerling, A. Wolf, U. Peschel, S. Höfling, C. Schneider, and S. Klemmt, Electro-optical Switching of a Topological Polariton Laser, *ACS Photonics* **2022**, *9*, 405–412.
- [29] S. Kéna-Cohen and S. R. Forrest, Room-temperature polariton lasing in an organic single-crystal microcavity, *Nat. Photonics* **2010**, *4*, 371.
- [30] J. D. Plumhof, T. Stöferle, L. Mai, U. Scherf, and R. F. Mahrt, Room-temperature Bose–Einstein condensation of cavity exciton–polaritons in a polymer, *Nat. Mater.* **2014**, *13*, 247 (2014).
- [31] C. P. Dietrich, A. Steude, L. Tropsch, M. Schubert, N. M. Kronenberg, K. Ostermann, S. Höfling, M. C. Gather, An exciton-polariton laser based on biologically produced fluorescent protein, *Sci. Adv.*, **2016**, *2*, e1600666.
- [32] J. Keeling and S. Kéna-Cohen, Bose–Einstein Condensation of Exciton- Polaritons in Organic Microcavities, *Annu. Rev. Phys. Chem.* **2020**, *71*, 435.
- [33] X. Liu, T. Galfsky, Z. Sun, F. Xia, E.-C. Lin, Y.-H. Lee, S. Kéna-Cohen, and V. M. Menon, Strong light–matter coupling in two-dimensional atomic crystals. *Nat. Photon.* **2015**, *9*, 30–34.
- [34] S. Dufferwiel, S. Schwarz, F. Withers, A. A. P. Trichet, F. Li, M. Sich, O. Del Pozo-Zamudio, C. Clark, A. Nalitov, D. D. Solnyshkov, G. Malpuech, K. S. Novoselov, J. M. Smith, M. S. Skolnick, D. N. Krizhanovskii, and A. I. Tartakovskii, Exciton–polaritons in van der Waals heterostructures embedded in tunable microcavities. *Nat. Commun.* **2015**, *6*, 8579.
- [35] N. Lundt, S. Klemmt, E. Cherotchenko, S. Betzold, O. Iff, A. V. Nalitov, M. Klaas, C. P. Dietrich, A. V. Kavokin, S. Höfling, and C. Schneider, Room-temperature Tamm-plasmon exciton–polaritons with a WSe₂ monolayer. *Nat. Commun.* **2016**, *7*, 13328.
- [36] K. F. Mak and J. Shan, Photonics and optoelectronics of 2D semiconductor transition metal dichalcogenides. *Nat. Photon.* **2016**, *10*, 216–226.

- [37] A. Brehier, R. Parashkov, J.-S. Lauret, and E. Deleporte, Strong exciton-photon coupling in a microcavity containing layered perovskite semiconductors. *Appl. Phys. Lett.* **2006**, *89*, 171110.
- [38] R. Su, C. Diederichs, J. Wang, T. C. H. Liew, J. Zhao, S. Liu, W. Xu, Z. Chen, and Q. Xiong, Room-temperature polariton lasing in all-inorganic perovskite nanoplatelets. *Nano Lett.* **2017**, *17*, 3982–3988.
- [39] A. Fieramosca, L. Polimeno, V. Ardizzone, L. De Marco, M. Pugliese, V. Maiorano, M. De Giorgi, L. Dominici, G. Gigli, D. Gerace, D. Ballarini, and D. Sanvitto, Two-dimensional hybrid perovskites sustaining strong polariton interactions at room temperature. *Sci. Adv.* **2019**, *5*, eaav9967.
- [40] K. Łempicka-Mirek, M. Król, H. Sigurdsson, A. Wincukiewicz, P. Morawiak, R. Mazur, M. Muszyński, W. Piecek, P. Kula, T. Stefaniuk, M. Kamińska, L. De Marco, P. G. Lagoudakis, D. Ballarini, D. Sanvitto, J. Szczytko, B. Piętka, Electrically tunable Berry curvature and strong light-matter coupling in liquid crystal microcavities with 2D perovskite, *Sci. Adv.* **2022**, *8*, eabq7533.
- [41] R. Jayaprakash, C. E. Whittaker, K. Georgiou, O. S. Game, K. E. McGhee, D. M. Coles, and D. G. Lidzey, Two-Dimensional Organic-Exciton Polariton Lattice Fabricated Using Laser Patterning, *ACS Photonics* **2020**, *7*, 2273–2281.
- [42] F. Scafirimuto, D. Urbonas, M. A. Becker, U. Scherf, R. F. Mahrt, and T. Stöferle, Tunable exciton–polariton condensation in a two-dimensional Lieb lattice at room temperature, *Communications Physics* **2021**, *4*, 39.
- [43] J. Wu, S. Ghosh, Y. Gan, Y. Shi, S. Mandal, H. Sun, B. Zhang, T. C. H. Liew, R. Su, Q. Xiong, Higher-order topological polariton corner state lasing. *Sci. Adv.* **2023**, *9*, eadg4322.
- [44] O. Shimomura, The discovery of aequorin and green fluorescent protein. *Journal of Microscopy* **2005**, *217*, 3-15.
- [45] M. Dusel, S. Betzold, O. A. Egorov, Room temperature organic exciton–polariton condensate in a lattice, *Nat. Commun.* **2020**, *11*, 2863.
- [46] M. Dusel, S. Betzold, T. H. Harder, M. Emmerling, J. Beierlein, J. Ohmer, U. Fischer, R. Thomale, C. Schneider, S. Höfling, and S. Klemmt, Room-Temperature Topological Polariton Laser in an Organic Lattice, *Nano Lett.* **2021**, *21*, 6398–6405.
- [47] A. H. Castro Neto, F. Guinea, N. M. R. Peres, K. S. Novoselov, and A. K. Geim, The electronic properties of graphene, *Rev. Mod. Phys.* **2009**, *81*, 109.

- [48] S. Y. Zhou, G.-H. Gweon, A. V. Fedorov, P. N. First, W. A. de Heer, D.-H. Lee, F. Guinea, A. H. Castro Neto & A. Lanzara, Substrate-induced bandgap opening in epitaxial graphene, *Nature Materials* **2007**, *6*, 770–775.
- [49] S. Klemmt, T. H. Harder, O. A. Egorov, K. Winkler, H. Suchomel, J. Beierlein, M. Emmerling, C. Schneider, S. Höfling, Polariton condensation in S- and P-flatbands in a two-dimensional Lieb lattice, *Appl. Phys. Lett.* **2017**, *111*, 231102.
- [50] C. E. Whittaker, E. Cancellieri, P. M. Walker, D. R. Gulevich, H. Schomerus, D. Vaitiekus, B. Royall, D. M. Whittaker, E. Clarke, I. V. Iorsh, I. A. Shelykh, M. S. Skolnick, and D. N. Krizhanovskii, Exciton Polaritons in a Two-Dimensional Lieb Lattice with Spin-Orbit Coupling, *Phys. Rev. Lett.* **2018**, *120*, 097401.
- [51] T. H. Harder, O. A. Egorov, C. Krause, J. Beierlein, P. Gagel, M. Emmerling, C. Schneider, U. Peschel, S. Höfling, and S. Klemmt, Kagome Flatbands for Coherent Exciton-Polariton Lasing, *ACS Photonics* **2021**, *8*, 3193–3200.
- [52] B. Real, O. Jamadi, M. Milićević, N. Pernet, P. St-Jean, T. Ozawa, G. Montambaux, I. Sagnes, A. Lemaître, L. Le Gratiet, A. Harouri, S. Ravets, J. Bloch, and A. Amo, Semi-Dirac Transport and Anisotropic Localization in Polariton Honeycomb Lattices, *Phys. Rev. Lett.* **2020**, *125*, 186601.
- [53] T. H. Harder, PhD Thesis, University of Würzburg, urn:nbn:de:bvb:20-opus-259008, February, **2022**.
- [54] S. Betzold, M. Dusel, O. Kyriienko, C. P. Dietrich, S. Klemmt, J. Ohmer, U. Fischer, I. A. Shelykh, C. Schneider, and S. Höfling, Coherence and Interaction in Confined Room-Temperature Polariton Condensates with Frenkel Excitons, *ACS Photonics* **2020**, *7*, 384–392.
- [55] T. Yagafarov, D. Sannikov, A. Zasedatelev, K. Georgiou, A. Baranikov, O. Kyriienko, I. Shelykh, L. Gai, Z. Shen, D. Lidzey, and P. Lagoudakis Mechanisms of blueshifts in organic polariton condensates, *Commun. Phys.* **2020**, *3*, 18.
- [56] L. Lackner, M. Dusel, O. A. Egorov, B. Han, H. Knopf, F. Eilenberger, S. Schröder, K. Watanabe, T. Taniguchi, S. Tongay, C. Anton-Solanas, S. Höfling, and C. Schneider, Tunable exciton-polaritons emerging from WS₂ monolayer excitons in a photonic lattice at room temperature. *Nat. Commun.* **2021**, *12*, 4933.
- [57] N. Tomm, A. Javadi, N. O. Antoniadis, D. Najer, M. C. Löbl, A. R. Korsch, R. Schott, S. R. Valentin, A. D. Wieck, A. Ludwig, and R. J. Warburton, A bright and fast source of coherent single photons, *Nat. Nanotechnol.* **2021**, *16*, 399-403.